

## Atypical viscous fracture of human femurs

Zohar Yosibash<sup>\*1</sup>, Romina Plitman Mayo<sup>1</sup> and Charles Milgrom<sup>2</sup>

<sup>1</sup>Department of Mechanical Engineering, Ben-Gurion University of the Negev, Beer-Sheva, 84105, Israel

<sup>2</sup>Hadassah Hospital and Hebrew University of Jerusalem, Ein-Kerem, Jerusalem, Israel

(Received January 12, 2014, Revised March 28, 2014, Accepted April 3, 2014)

**Abstract.** Creep phenomenon at the scale of bone tissue (small specimens) is known to be present and demonstrated for low strains. Here creep is demonstrated on a pair of fresh-frozen human femurs at the organ level at high strains. Under a constant displacement applied on femur's head, surface strains at the upper neck location increase with time until fracture, that occurs within 7-13 seconds. The monotonic increase in strains provides evidence on damage accumulation in the interior (probably damage to the trabeculae) prior to final fracture, a fact that hints on probable damage of the trabecular bone that occurs prior to the catastrophic fracture of the cortical surface layer.

**Keywords:** femur; fracture; creep

---

### 1. Introduction

Bone tissue exhibits both viscous effects as well as creep and stress relaxation Lakes *et al.* (1979). For example, several studies have been reported on the creep behavior of both trabecular and cortical bone tissue (for trabecular see Zilch *et al.* (1980), Bowman *et al.* (1994), and for cortical see Fondrk *et al.* (1988), Caler and Carter (1989)). Recent studies attempt to consider long-term bone creep effects to analyze the aseptic loosening of cemented prosthesis in femurs Norman *et al.* (2013) and creep phenomena in vertebral bones Luo *et al.* (2012). The creep phenomenon is characterized by creep strain vs time curves that have three distinct regimes and by several possible power law relationships between applied stress, time-to-failure, and steady-state creep rate. Many of these relationships are similar to those for conventional engineering materials such as metals (tensile creep) and ceramics (compressive creep).

The viscous and creep effects are insignificant for short time scales in the orders of seconds and at moderately low strain levels. Therefore, patient-specific finite element (FE) models based on CT scans that become extensively popular for predicting the mechanical response and failure loads in long bones, disregard these time dependent effects and consider time-independent constitutive laws, see e.g., Keyak *et al.* (1990), Viceconti *et al.* (2004), Schileo *et al.* (2007), Bessho *et al.* (2007), Yosibash *et al.* (2007a, b), Trabelsi *et al.* (2009). In-vitro experiments aimed at validating the FE models are usually performed, during which fresh-frozen femurs are defrosted, instrumented by strain-gauges and loaded monotonically until fracture. Such experiments are

---

\*Corresponding author, Professor, E-mail: [zohary@bgu.ac.il](mailto:zohary@bgu.ac.il)

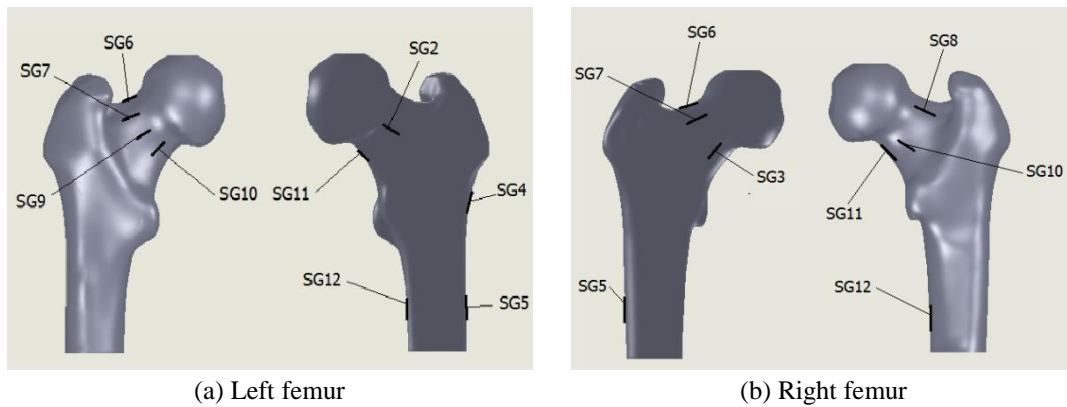


Fig. 1 The two proximal femurs and SGs locations

inappropriate for the investigation of creep effects, and to the best of our knowledge the effect of creep on the fresh-frozen femur-level has not yet been investigated, especially at high strains. We here provide experimental evidence on the strong influence of creep leading to fracture (time-dependent) phenomena at the femur level. Furthermore, the creep effect at high strains may explain qualitatively the fracture initiation evolution, a topic which is under continuous debate and investigation.

## 2. Materials and methods

A pair of femurs harvested from a 77 years old, 180 cm high, 50 kg Caucasian male donor, that deceased due to lung cancer, were deep-frozen after harvest and thawed at room temperature on the day of the experiment. Soft tissue was removed from the bone by a combination of sharp and blunt dissection. The femurs were then cut to about 250 mm and the proximal parts were mounted into cylindrical steel devices. The mounting jig is documented in Yosibash *et al.* (2007a). The left femur had a relatively medium sized tumor of the type adenocarcinoma in the head and lower part of the neck whereas the right femur had a very small tumor in the middle of the neck (determined by histopathology inspections after fracture).

Thirteen uniaxial strain gauges (SGs) (Vishay general purpose uniaxial SGs with a sensitivity of  $\pm 0.2\%$ ) were bonded to the superior and inferior neck and the medial and lateral shaft, using M-Bond 200 Cyanoacrylate Adhesive (Measurements Group, Inc., Raleigh, NC, USA) (see SG distribution in Fig. 1). The SGs were bonded so to align with the assumed local principal strain directions which could only be validated in a finite-element analysis at the post process phase. Three Vishay linear displacement sensors (LDS, precision of  $\pm 0.2\%$ ) were used to measure displacements at two locations. Vishay system 7000 combined with Strain-Smart software was used to record the output data from the load cell (via an amplifier), SGs and LDS. The femurs were kept overnight in a humid container in a refrigerator until the next morning at which the mechanical experiments were performed.

A displacement driven compression machine Zwick 1445 (Zwick GmbH & Co. KG., Germany 1992) was used that applied displacements at a rate of 16.67 mm/sec, while monitoring the load. A load cell with a saturation level of 12,000 Newton was used to measure the load. A flat and smooth

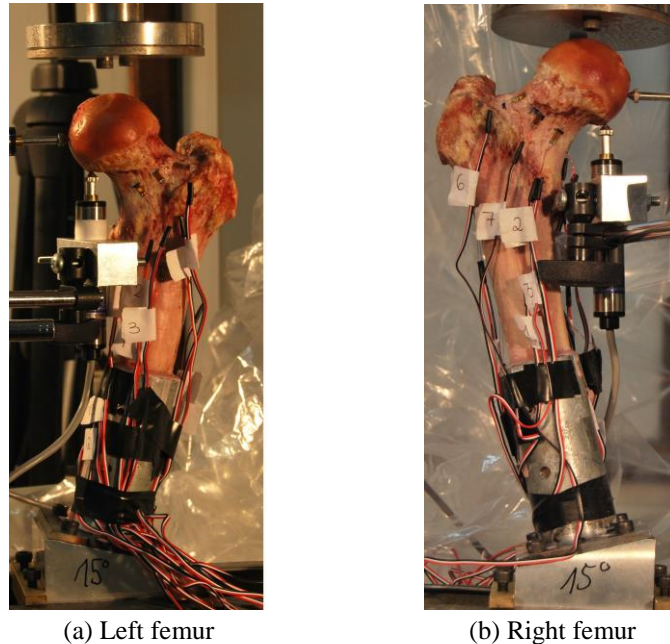


Fig. 2 The experimental setup

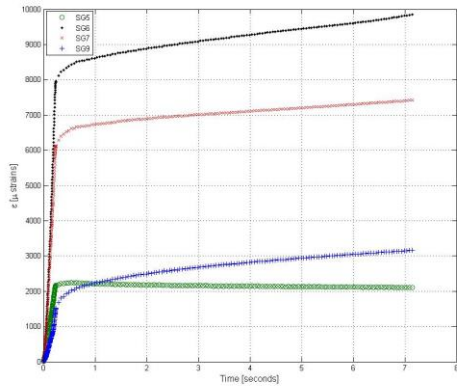
aluminum plate applied the displacement directly to femur's head. Prior to the fracture experiment, loads of low magnitudes (up to 1000 N) were applied to the femurs at three inclination angles  $0^\circ$ ,  $7^\circ$  and  $15^\circ$  which showed a linear response (SGs showed zero strains after removal of the load). The femurs were finally inclined at  $15^\circ$  as shown in Fig. 2, and a displacement on their head was applied.

The right femur's upper part of the head was subjected to a displacement of 3.7 mm and the left femur to a displacement of 3.2 mm (at a rate of 16.67 mm/sec) and then the displacement was kept constant until fracture. Following fracture, a histopathology was performed to the broken heads to identify the metastatic tumors and their magnitude.

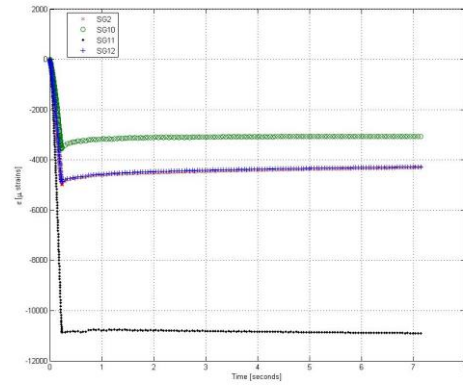
### 3. Results

A transcervical fracture occurred in the left femur after 7.2 sec and a subcapital fracture in the right femur after 13.03 sec. The relevant SGs' output as a function of time (from the application of the displacement until fracture) is presented in Figure 3 for the left femur and in Fig. 4 for the right femur.

The saturation level of the load cell is 12,000 N, so that applied displacement rate is terminated when this load is reached and thereafter the reached displacement (applied on the femurs' head) is kept constant. In Fig. 5 we present the relative displacement (applied displacement over the maximum displacement) and the relative force on the right and left femurs as a function of time until fracture. Fig. 6 shows the fractured femurs on which the mid-plane and histology with the tumor is superimposed. The maximum strains (tension or compression) measured by the SGs at the neck are summarized in Tables 1-2.

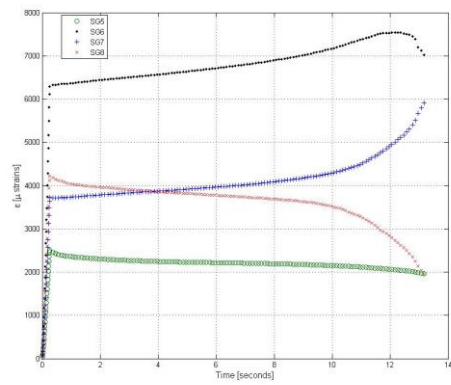


(a) SGs in tension

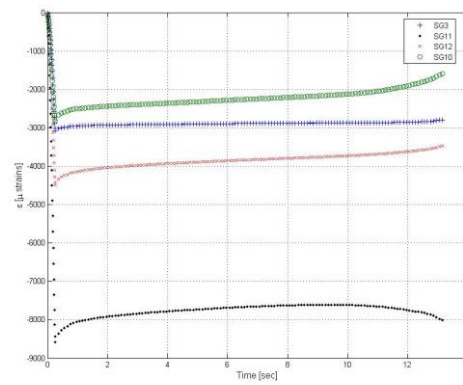


(b) SGs in compression

Fig. 3 Left femur - SG data ( $\mu$ strains)

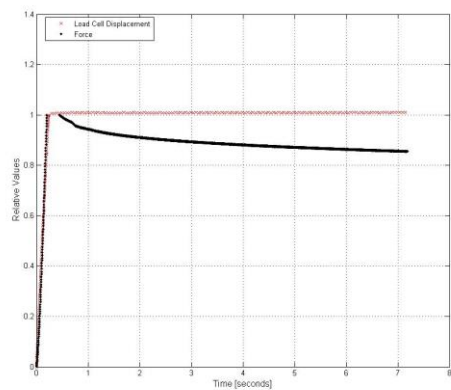


(a) SGs in tension

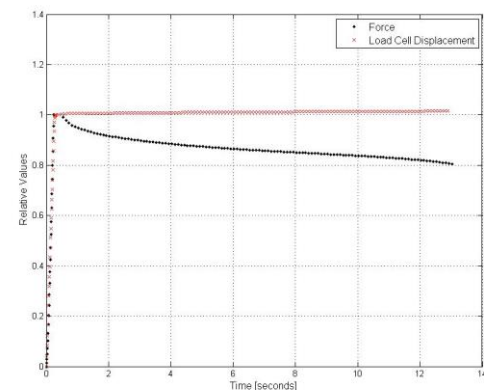


(b) SGs in compression

Fig. 4 Right femur - SG data ( $\mu$ strains)



(a) Left femur



(b) Right femur

Fig. 5 Relative applied displacement and resulting load on the femurs

Table 1 Strains in  $\mu$ strains - Right femur

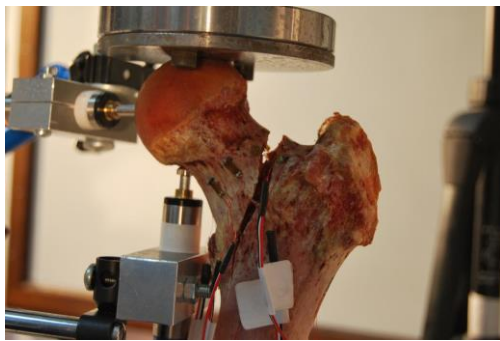
SG#	SG3	SG6	SG7	SG8	SG11
End elastic response (1)	-2730	5492	3307	3735	-7749
Maximum	-3079(2)	7545(3)	5988(4)	4253(2)	-8581(2)
Final ( $t=13.21s$ )	-2770	6992	5988	1928	-8003

(1) At  $t=0.23s$ , and load of (11706N), (2) Between  $t=0.23$  and  $t=0.43$ , which is the time the load cell stop recording, (3) Between  $t=0.43$  and fracture, (4) At fracture.

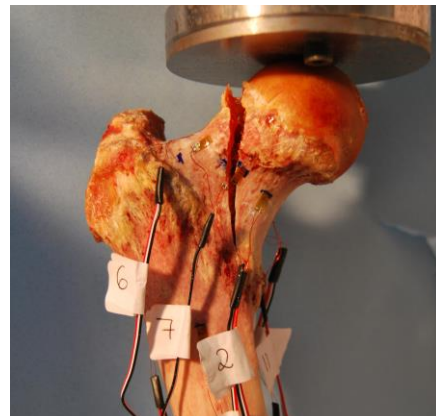
Table 2 Strains in  $\mu$ strains - Left femur

SG#	SG2	SG6	SG7	SG9	SG11
End elastic response (1)	-4427	6614	5076	1038	-9446
Maximum	-4982(2)	9873(3)	7433(3)	3175(3)	-10918(4)
Final ( $t=7.29s$ )	-4298	9862	7420	3154	-10916

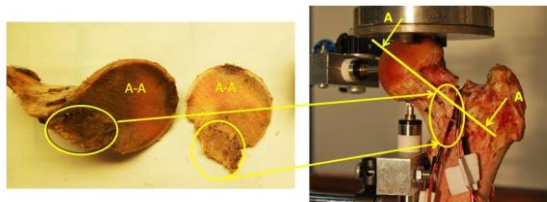
(1) At  $t=0.20s$ , and load of (11749N), (2) Between  $t=0.20$  and  $t=0.45$ , which is the time the load cell stop recording, (3) Between  $t=0.45$  and fracture, (4) At fracture.



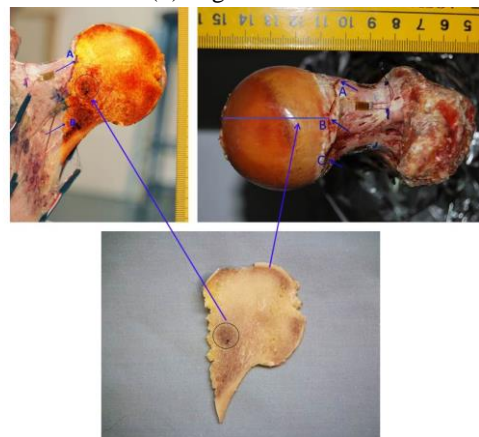
(a) Left femur



(b) Right femur



(c) Left - fracture with tumor



(d) Right - fracture with tumor

Fig. 6 The fractured femurs with location of tumor

#### 4. Conclusions

Although the creep phenomenon is known to be present in bone tissues and demonstrated for low strains at the tissue level (relatively small extracted specimens), it is not investigated or demonstrated at the organ level, and its influence is mostly ignored. In this study we have shown that creep is clearly visible at the organ level at high strains in femurs. At a given constant displacement applied on the femur's head all measured strains changed as a function of time, and the load decreased. The time to failure was relatively fast and occurred within 7-13 seconds. Since the experiments were displacement controlled, no visual evidence of the expected fracture was noticed until fracture.

Inspection of video films of the fracture process, and the SGs behavior as a function of time, provided evidence that in both femurs the fracture initiation occurred at the upper neck in tension. At this location the strain measured by SG6 (the closest SG to the anticipated starting point of the fracture on the surface) was the highest (among all other SGs) and increased as a function of time until fracture.

In the left femur, SG6 which is very close to the fracture path reached almost 10,000  $\mu$ strains just before fracture, well beyond the anticipated "yield strain" of 7300  $\mu$ strain Bayraktar *et al.* (2004). In the right femur, SG6 although being the closest to the fracture initiation location, it was still further away and reached 7500  $\mu$ strains just before fracture. The strain at the fracture location was not measured and is anticipated to be higher.

The fracture path is the typical path at which femurs, that are loaded in this configuration until fracture, break. The fracture path in the left femur is a bit shifted from the head to the neck region - this may be attributed to the existence of a tumor of the type adenocarcinoma (determined by histology inspections after the test).

In the left femur the strains in the neck at the upper posterior location increased with time whereas in the right femur, the strains in the upper anterior location increased with time. The monotonic increase in strains on the surface provided evidence on damage accumulation in the interior (probably damage to the trabeculae) prior to final fracture, a fact that hints on probable damage of the trabecular bone that occurs prior to the catastrophic fracture of the cortical surface layer.

During the loading stage all SG responded linearly until the maximum load. This phenomenon suggests that at the macroscopic level no damage accumulation is visible if the femurs are loaded at a high strain rate monotonically until fracture, and they behave linearly elastic until fracture. This observation coincides with Juszczak *et al.* (2011).

The limitations of the current study are: The maximum load was not measured due to the saturation level of the load cell at 12,000N. Tumors of the type adenocarcinoma are present (but very minor in the right femur) which may have an influence on the creep behavior.

#### Acknowledgements

We would like to thank Dr. Nir Trabelsi from Shamun College of Engineering, Israel, Mr. Ilan Gilad and Mr. Natan Levin from the Ben-Gurion University, Israel, and Mr. Hagen Wille from TUM, Germany for their help with the experiments. The first author gratefully acknowledges the generous support of the Technical University of Munich - Institute for Advanced Study, funded by the German Excellence Initiative. This study was supported in part by grant no. 3-00000-7375

from the Chief Scientist Office of the Ministry of Health, Israel.

## References

- Bayraktar, H., Morgan, E., Niebur, G., Morris, G., Wong, E. and Keaveny, M. (2004), "Comparison of the elastic and yield properties of human femoral trabecular and cortical bone tissue", *J. Biomech.*, **37**, 27-35.
- Bessho, M., Ohnishi, I., Matsuyama, J., Matsumoto, T., Imai, K. and Nakamura, K. (2007), "Prediction of strength and strain of the proximal femur by a CT-based finite element method", *J. Biomech.*, **40**, 1745-1753.
- Bowman, S.M., Keaveny, T., Gibson, J.L., Hayes, W. and McMahon, T.A. (1994), "Compressive creep behavior of bovine trabecula bone", *J. Biomech.*, **27**, 301-310.
- Caler, W.E. and Carter, D.R. (1989), "Bone creep-fatigue damage accumulation", *J. Biomech.*, **22**, 625-635.
- Fondrk, M., Bahniuk, E., Davy, D.T. and Michaels, C. (1988), "Some viscoplastic characteristics of bovine and human cortical bone", *J. Biomech.*, **21**, 623-630.
- Juszczyk, M.M., Cristofolini, L. and Viceconti, M. (2011), "The human proximal femur behaves linearly elastic up to failure under physiological loading conditions", *J. Biomech.*, **44**, 2259-2266.
- Keyak, J.H., Meagher, J.M., Skinner, H.B. and Mote, J.C.D. (1990), "Automated three dimensional finite element modelling of bone: A new method", *ASME J. Biomech. Eng.*, **12**, 389-397.
- Lakes, R., Katz, J. and Sternstein, S. (1979), "Viscoelastic properties of wet cortical bone I. Torsional and biaxial studies", *J. Biomech.*, **12**, 657-678.
- Luo, J., Pollintine, P., Gomm, E., Dolan, P. and Adams, M.A. (2012), "Vertebral deformity arising from an accelerated "creep" mechanism", *Eur. Spine J.*, **21**, 1684-1691.
- Norman, T.L., Shultz, T., Noble, G., Gruen, T.A. and Blaha, J.D. (2013), "Bone creep and short and long term subsidence after cemented stem total hip arthroplasty (THA)", *J. Biomech.*, **46**, 949-955.
- Schileo, E., Taddei, F., Malandrino, A., Cristofolini, L. and Viceconti, M. (2007), "Subject-specific finite element models can accurately predict strain levels in long bones", *J. Biomech.*, **40**, 2982-2989.
- Trabelsi, N., Yosibash, Z. and Milgrom, C. (2009), "Validation of subject-specific automated p-FE analysis of the proximal femur", *J. Biomech.*, **42**, 234-241
- Viceconti, M., Davinelli, M., Taddei, F. and Cappello, A. (2004), "Automatic generation of accurate subject-specific bone finite element models to be used in clinical studies", *J. Biomech.*, **37**, 1597-1605.
- Yosibash, Z., Padan, R., Joscowicz, L. and Milgrom, C. (2007a), "A CT-based high-order finite element analysis of the human proximal femur compared to in-vitro experiments", *ASME J. Biomech. Eng.*, **129**, 297-309
- Yosibash, Z., Trabelsi, N. and Milgrom, C. (2007b), "Reliable simulations of the human proximal femur by high-order finite element analysis validated by experimental observations", *J. Biomech.*, **40**, 3688-3699
- Zilch, H., Rohlmann, A., Bergmann, G. and Kolbel, R. (1980), "Material properties of femoral cancellous bone in axial loading. Part II: Time dependent properties", *Acta Orthop. Traumat. Surg.*, **97**, 257-262.